

Impact Damage Prediction for Wave Energy Converters

Ryan Meekins¹, Stephen Adams², Kevin Farinholt³, Nathan Hipwell⁴, Michael Desrosiers⁵, and Peter Beling⁶

^{1,2,6} *University of Virginia, Charlottesville, VA 22904, USA*

ryanmeekins@virginia.edu

sca2c@virginia.edu

beling@virginia.edu

^{3,4,5} *Luna Innovations Inc., Charlottesville, VA, 22903, USA*

farinholtk@lunainc.com

hipwelln@lunainc.com

desrosiersm@lunainc.com

ABSTRACT

Marine and hydrokinetic energy is of growing interest across the globe because it has the potential to provide a large source of renewable energy from the world's oceans and rivers. These marine and hydrokinetic devices, such as wave energy converters, must operate remotely in all weather conditions, including severe storms. Thus, these devices can suffer from structural damage affecting their performance and lifespan. Therefore, there is interest in developing structural health monitoring systems that can identify new damage, estimate its severity, and then make a decision to provide crews with a maintenance or control recommendation. In this study, we investigate using the electromechanical impedance response of piezoelectric transducers to actively monitor the structural health of composite materials similar to those used in several marine and hydrokinetic devices. Recurring impact damage experiments were completed on five plates using a test drop stand, consisting of five consecutive impacts at the same location for each plate. Classification and regression methods were evaluated in an attempt to predict impact damage on a new plate. Machine learning algorithms were used on data collected over a frequency range of 10 kHz to 100 kHz for two types of piezoelectric transducers.

1. INTRODUCTION

Marine and hydrokinetic (MHK) devices are one of the newest and fastest growing renewable energy technologies (Yuce & Muratoglu, 2015). The Department of Energy (DOE) estimates that MHK devices could theoretically provide the United States with up to 42% of its electricity (DOE,

2016). A subset of these devices that promise to provide the largest proportion of energy is the wave energy converter (WEC). WECs generate electricity from the movement of ocean surface waves. A full review of WEC technology can be found in (Antonio, 2010). A major obstacle to widespread implementation of WECs is their economic feasibility (Lehmann, Karimpour, Goudey, Jacobson, & Alam, 2017).

To decrease energy production costs and to increase energy harvesting efficiency, researchers are currently optimizing WEC designs and operations. The DOE's recent Wave Energy Prize (EERE, 2017), which awarded 6.5 million dollars to top design teams, has demonstrated the acceleration of WEC technology. Four teams surpassed the DOE's "state of the art" technology goal, with the winning team demonstrating a five-fold improvement in WEC technology. The DOE's goal metric accounts to WECs having a high energy harvesting efficiency and a low cost of production, which would lead to a reduced levelized cost of electricity (LCOE).

Early sea trials of WEC devices have also found them to be damaged by their environmental conditions, resulting from exposure to unforeseen loadings. Therefore, in order to produce WECs of low cost and that survive the harsh sea environments, current WEC manufacturers are experimenting with using structural health monitoring (SHM). SHM could be used to optimize operating decisions, including maintenance and repair activities and control decisions, leading to a lower LCOE.

WEC structures are generally manufactured using fiber reinforced plastic (FRP) composites because of their low cost, high strength, and resistance to corrosion. FRPs are of growing interest in aerospace, renewable energy, and many other fields because of these properties. All structures are sus-

Ryan Meekins et al. This is an open-access article distributed under the terms of the Creative Commons Attribution 3.0 United States License, which permits unrestricted use, distribution, and reproduction in any medium, provided the original author and source are credited.

ceptible to damage and due to the emerging trend of using FRPs, it is of great interest to be able to monitor the health of these composite structures. This structural health monitoring would potentially extend the life of these devices by providing efficient maintenance decisions and optimized control decisions. These decisions would lead to an increased system resilience and savings in time and money.

FRP structures can fail from fiber breakage, matrix cracking, and delamination. Piezoelectric transducers can be used to collect impedance response signals on the FRP structure of WECs. The goal of our research is to design machine learning algorithms for estimating the structural health of WEC composite structures. The work presented in this study is a continuation of the work presented in (Farinholt et al., 2016), in particular, the discrete damage plate experiments.

In the previous study, an FRP plate was damaged by cutting and drilling into the material. It was demonstrated that the impedance measurements from the piezoelectric transducers could be used in conjunction with machine learning algorithms to estimate the discrete damage case. However, the experiments in (Farinholt et al., 2016) are limited to a single plate. In the presented study, five plates are damaged in order to characterize cross-plate variation. Further, the experimental setup is refined by using a drop stand to impact realistic damage to each composite plate.

Our initial assumption was that the drop stand would damage each plate in a similar fashion and that each impact would represent a separate damage class. However, we discovered a large amount of variation across plates in both the damage delivered by the drop stand and the corresponding change in response collected by the piezoelectric transducers. From this observation, we conclude that the task at hand is a regression problem with a continuous dependent variable as opposed to a classification problem with nominal classes. We perform several sets of numerical experiments to justify this conclusion. Further, we demonstrate that predictive models are not transferable across plates, i.e. a model trained on one plate would not necessarily be able to predict damage on another plate, because the changes in the frequency responses due to damage are not consistent across plates.

This paper is organized in the following manner: Section 2 provides background information in the field of SHM for composites. Section 3 describes the experimental setup and collected data. Section 4 describes the classification analysis, with multi-class and binary class classification problems explored and evaluated using two types of validation methods. Section 5 describes the creation of a regression problem and the results. Section 6 provides our conclusion with a discussion of sources of error and plans for future work.

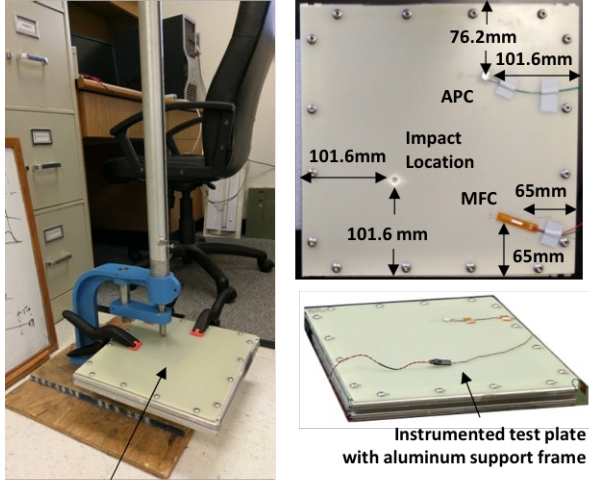
2. BACKGROUND

This research focuses on using the electromechanical impedance (EMI) technique for structural health monitoring (SHM). The EMI technique is presented in (Park & Inman, 2007), which also includes an applied example to concrete SHM. The EMI technique is a vibration based method which relies on damage changing a materials mechanical properties, which are then detected by changes in the electrical impedance of a bonded transducer. The EMI technique has been recently used for the SHM of concrete in (Xie, Xu, Guo, Sha, & Huang, 2016; Xu, Banerjee, Wang, Huang, & Cheng, 2015; Dumoulin, Karaiskos, Sener, & Deraemaeker, 2014) and the SHM of wind turbines in (Taylor et al., 2014; Yoon, He, & Van Hecke, 2015), as well as many other fields. In our experiments, the EMI technique is used with lead zirconate titanate (PZT) piezoelectric transducers for the SHM of WEC composites.

Many other groups have recently studied SHM of composites that focused on impact damage. Three carbon-fiber reinforced plastic (CFRP) plates were impacted and detected using two piezoelectric transducers, one that actuates and one that detects in (Nardi, Lampani, Pasquali, & Gaudenzi, 2016). Auto-regressive (AR) models were used to predict the presence of a new impact damage, with higher order AR models predicting the damage case 100% of the time. A fiber Bragg grating (FBG) transducer network was used to locate impacts in (Frieden, Cugnoni, Botsis, & Gmür, 2012b) and then to predict impact damage size in (Frieden, Cugnoni, Botsis, & Gmür, 2012a). Their iterative optimization algorithm, which relies on knowing the impact location, estimates damage size to within 30%. An extensive impact damage study which included 48 CFRP plates was conducted using vibration-based methods in (Pérez, Gil, & Oller, 2014). This paper relates the damage identification to the plates reduction in strength, with the earliest detection of damage at 27% reduction in strength.

3. EXPERIMENTAL SETUP

A series of experiments were conducted using five Garolite G-10 test panels that are fabricated from an epoxy resin infused within a fiberglass reinforcement fabric. Each panel was mounted to an aluminum reinforcement frame using sixteen $\frac{1}{4}$ "-20 machine screws that were tightened to 4 Nm of torque prior to each experiment, as shown in Fig. (1). The laminate plates were instrumented with a single 9.55 mm x 1 mm piezoelectric disk transducer manufactured by APC International, Ltd from their 850 type piezoceramic material, as well as a 25 mm x 3 mm P1 type Macro Fiber Composite (MFC) transducer from Smart Material Corp. Transducers were mounted using Loctite's model 234790 cyanoacrylate gel adhesive, with constant pressure applied for 30 seconds during the bonding process. Baseline impedance measurements were collected using a Hioki IM3533-01 impedance,



Drop test stand used to impact composite plates to introduce penetration damage and delamination within the laminate

Figure 1. The experimental setup including the mounted plate with transducers and the impact test stand.

current, resistance (LCR) meter. Data was collected over a frequency range of 10 kHz to 100 kHz for the real and imaginary components of the transducer's electrical impedance. A total of 10 data points were collected at each frequency and averaged, with a step in frequency of 50 Hz. Once baseline conditions were measured, the test panels were inserted in a drop test stand, shown in Fig. (1), and subject to impact events using a tapered impactor positioned 101.6 mm from one corner of the G-10 panels. Each plate was subject to five sequential impacts using a 3.6 kg mass dropped from a height of 0.381 m. Five impedance scans were collected after each impact event. The five recurring impact events represent the five different damage severities used to train the machine learning models.

In addition to collecting the impedance scans, optical images of the impact damages were collected while the plate was illuminated using a high intensity LED lighting fixture. Fig. (2) shows these images for plate 4 and illustrates the increasing level of damage observed after each strike to the plate.

3.1. Data

Five recurring impacts were completed on five plates. For each plate's baseline and plate's impact number, five impedance scans were collected from both transducers. This resulted in 150 observations per transducer (5 plates * (1 baseline + 5 impacts) * 5 scans), however, one impact observation from the MFC transducer was left out because the LCR meter failed to collect across the full frequency range.

The data collected from plate 4 using both APC and MFC transducers is shown in Fig. (3). This figure shows each damage class plotted as a different color and shows the dif-

ferences between the APC and MFC transducer responses. The APC transducer results in more dynamic content across the frequency band, with peaks of a larger proportional height to the full response. The data collected from plates 2 and 4 are shown in Fig. (4). This figure shows the regions of highest activity, between 10 and 20 kHz for both transducers. The APC transducer plot shows the distinct differences in the responses between the plates.

The machine learning features for each observation included various functions on an array that consisted of a sum of differences between the observations response and the observation plate's baseline responses at each frequency. This array of a sum of differences was calculated for the real and imaginary response data using Eq. (1) at each frequency,

$$\sum_{baseline=1}^5 r_{baseline} - r_{obs} \quad (1)$$

where r is the real or imaginary response at each frequency. The following features were extracted from this array of summed differences for each observation for both the real and imaginary impedance measurements: mean, standard deviation, variance, skewness, kurtosis, minimum, maximum, range, 1-norm, 2-norm, 3-norm, and infinity-norm.

4. CLASSIFICATION ANALYSIS

In this section, we describe the numerical experiments involving classification algorithms. The classification problem consists of six classes: baseline, impact 1, impact 2, impact 3, impact 4, and impact 5. We conducted two types of validation experiments, a leave-one-out cross validation (LOOCV) and a leave-one-plate-out cross validation (LOPOCV). LOPOCV is a testing methodology where all data from a single plate is reserved for testing, and the classifier is trained on the data from the four remaining plates. This cross validation technique was created to simulate damage prediction on a new and unseen plate. Based on our previous work in (Farinholt et al., 2016), we evaluate the classification tree (Bishop, 2006) and random forest algorithms (Breiman, 2001) for both LOOCV and LOPOCV.

4.1. Leave-One-Out Cross Validation

LOOCV using a classification tree results in 69% and 51% accuracy for the APC and MFC transducer data, respectively. A LOOCV using random forest with 500 trees resulted in 78% and 63% accuracy for the APC and MFC transducer data, respectively.

The confusion matrices for the LOOCV results using a classification tree and random forest with 500 trees are shown in Tab. (1) and Tab. (2), respectively. There are several conclusions that can be made from this initial set of numeri-

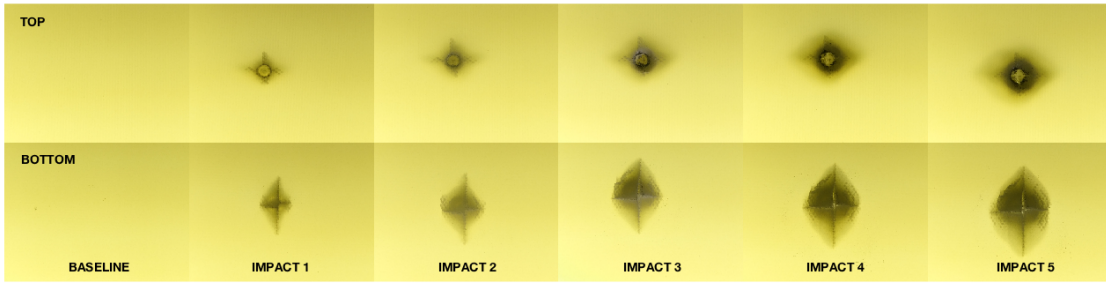


Figure 2. Backlit images of impact damage introduced to G-10 plate 4 using a drop test stand.

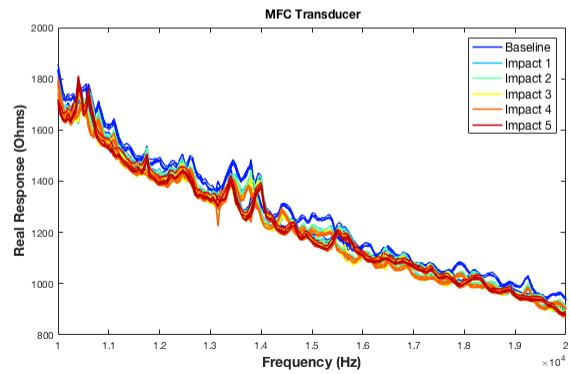
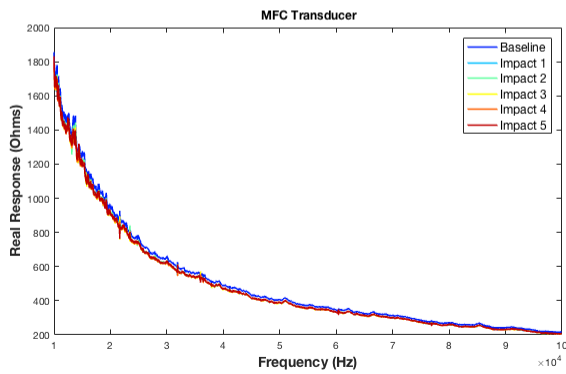
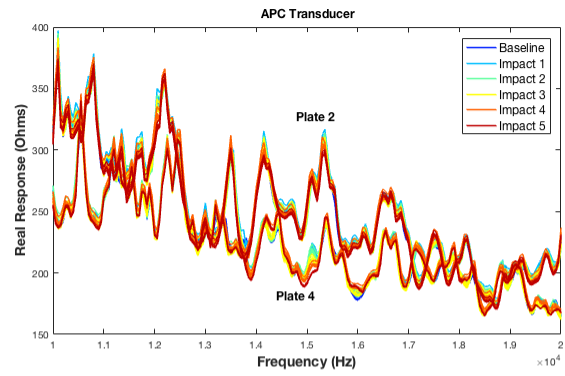
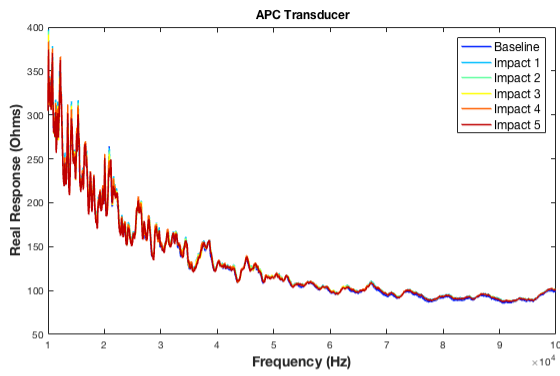


Figure 3. Real impedance responses from plate 4 using both APC and MFC transducers.

Figure 4. Real impedance responses from plates 2 and 4 using both APC and MFC transducers.

cal experiments. First, we have confirmed the result from (Farinholt et al., 2016) that random forest yields a high prediction accuracy. Second, these experiments demonstrate that given enough relevant data, machine learning algorithms can estimate the structural health class of a FRP plate with data collected from a piezoelectric transducer. However, this experimental design assumes that data from all plates and damage classes are available during training. Third, the data from APC transducer yields better results than the data from the MFC transducer.

Table 1. Confusion matrix for LOOCV using a classification tree with APC transducer data.

	Predicted Class					
	B	I1	I2	I3	I4	I5
Baseline	23	2	0	0	0	0
Impact 1	0	19	3	2	1	0
Impact 2	1	6	10	6	2	0
Impact 3	0	2	7	15	1	0
Impact 4	0	1	1	1	18	4
Impact 5	0	0	0	0	7	18

Table 2. Confusion matrix for LOOCV using random forest with APC transducer data.

	Predicted Class					
	B	I1	I2	I3	I4	I5
Baseline	24	1	0	0	0	0
Impact 1	0	20	3	1	1	0
Impact 2	0	6	13	5	1	0
Impact 3	0	1	3	19	2	0
Impact 4	0	1	0	2	18	4
Impact 5	0	0	0	0	2	23

4.2. Leave One Plate Out Cross Validation

LOPOCV using a classification tree resulted in 43% and 40% accuracy for the APC and MFC transducer data, respectively. These results are shown in Fig. (5). LOPOCV with random forest with 500 grown trees resulted in 42% and 33% accuracy for the predicted left out plate observations for the APC and MFC transducer data, respectively. These results are shown in Fig. (6). These figures show the accuracy of predicting the left out plate's classes for each plate and each transducer type.

The confusion matrix for the LOPOCV results using classification tree with the APC data is shown in Tab. (3). The confusion matrix for the LOPOCV results using random forest with 500 trees is shown in Tab. (4). Clearly, these classifiers are not transferable across plates.

4.3. Frequency Importance

In an effort to improve the performance of the classifiers, we attempted to select a relevant frequency range for use with the

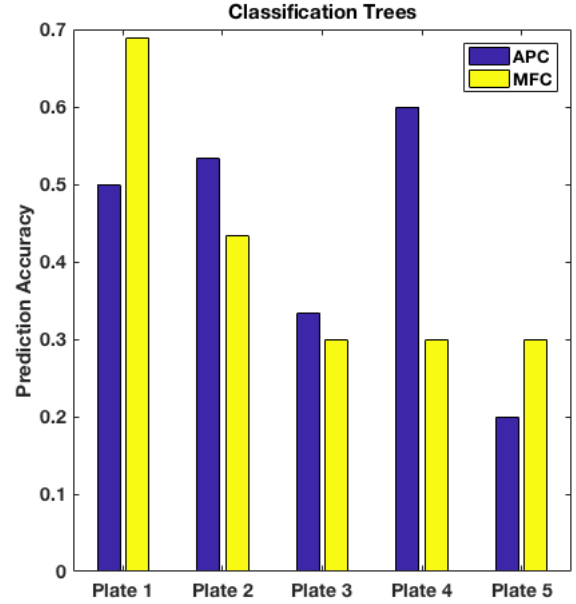


Figure 5. LOPOCV results using classification trees.

Table 3. Confusion matrix for LOPOCV using classification trees with APC transducer data.

	Predicted Class					
	B	I1	I2	I3	I4	I5
Baseline	23	1	1	0	0	0
Impact 1	0	10	7	7	1	0
Impact 2	0	15	1	7	2	0
Impact 3	0	7	8	6	4	0
Impact 4	0	7	0	5	5	8
Impact 5	0	1	0	0	4	20

classification algorithms. Variable importance was produced using a random forest classifier using the full real response array of summed differences from Eq. (1) for all observations for each plate and each transducer type.

This variable importance metric is calculated for each frequency or feature by removing the feature across all trees and then calculating the change in the out-of-bag error rate. MATLAB returns this change in error divided by the standard deviation. Removal of important features will cause the error to increase more than less important features. The resulting frequency importance was normalized and is shown for the entire frequency range in Fig. (7). This figure shows that the lower frequency range, from 10 kHz to 30 kHz may be the most important for classification.

This frequency importance metric was recalculated using a random forest model that excluded responses for frequencies above 30 kHz, in order to focus on this more important frequency range. The frequency importance is shown in Fig (8).

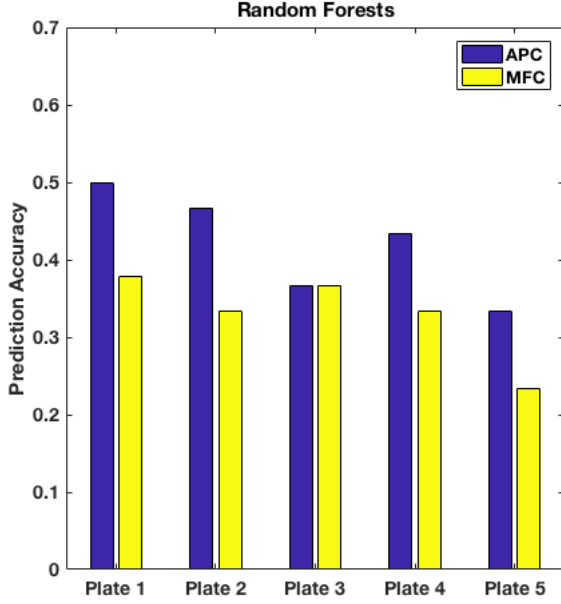


Figure 6. LOPOCV results using random forest with 500 trees.

Table 4. Confusion matrix for LOPOCV using random forest with APC transducer data.

	Predicted Class					
	B	I1	I2	I3	I4	I5
Baseline	24	0	1	0	0	0
Impact 1	1	8	7	9	0	0
Impact 2	0	10	0	10	5	0
Impact 3	0	5	4	8	8	0
Impact 4	0	2	0	6	8	9
Impact 5	0	0	0	0	10	15

These figures, however, show that overall, there are not frequencies or frequency ranges that are consistently important for classification for each plate. This would mean that it is very difficult to predict impact damage on an unseen plate using the full frequency response.

The LOPOCV analysis was evaluated using the array features for this low frequency range, with 41% and 23% accuracy for the classification tree for the APC and MFC transducer data, respectively, and 41% and 33% accuracy using the random forest model with 500 trees for the APC and MFC transducer data, respectively. This frequency range selection resulted in a slightly worse prediction accuracy, compared to using the full frequency range.

4.4. Binary Classification Problem

Given the previous results, we conclude that data for each plate must be incorporated into the training process. We re-

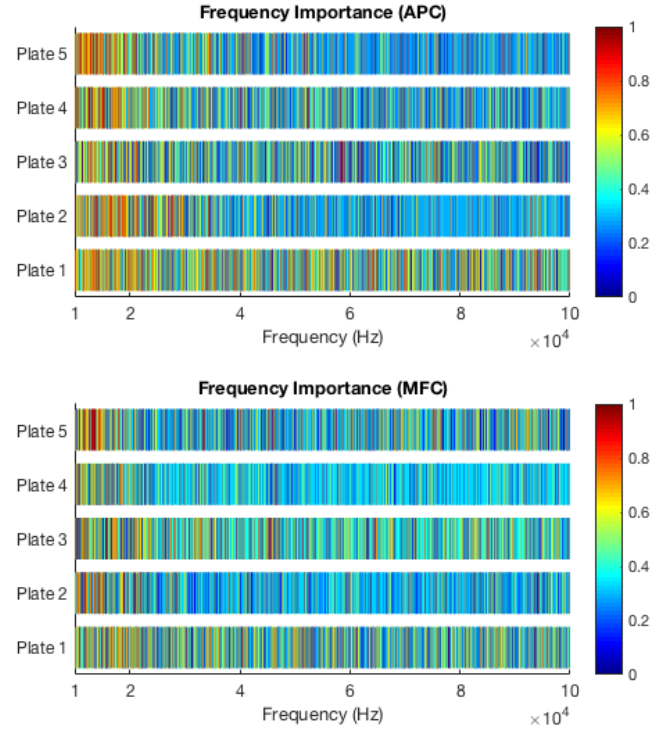


Figure 7. Frequency importance for each plate using random forest with 500 trees.

formulate the problem to binary classification, where we distinguish between a baseline and a damaged plate. We further change the problem by limiting the training procedure to only the baseline and constructing a separate model for each plate. Only plates with all five damage impacts are used in this evaluation.

We use a one class Naive Bayes model where each frequency is modeled as an independent Gaussian distribution. The log-likelihood of the impedance measurement can be calculated by

$$LL = \sum_{l=1}^L \log[\mathcal{N}(x_l | \mu_l, \sigma_l)], \quad (2)$$

where x_l is the impedance measurement at the l^{th} frequency for $l = 1 \dots L$, μ_l is the mean of the Gaussian distribution, and σ_l is the standard deviation of the l^{th} frequency. The mean and standard deviations are calculated from the baseline measurements for each plate. A threshold t is selected. The current measurement is classified as a baseline if $LL \geq t$ and as damaged if $LL < t$. The difficulty with this problem formulation is selecting the value of t . For this example, we select $t = -10^4$.

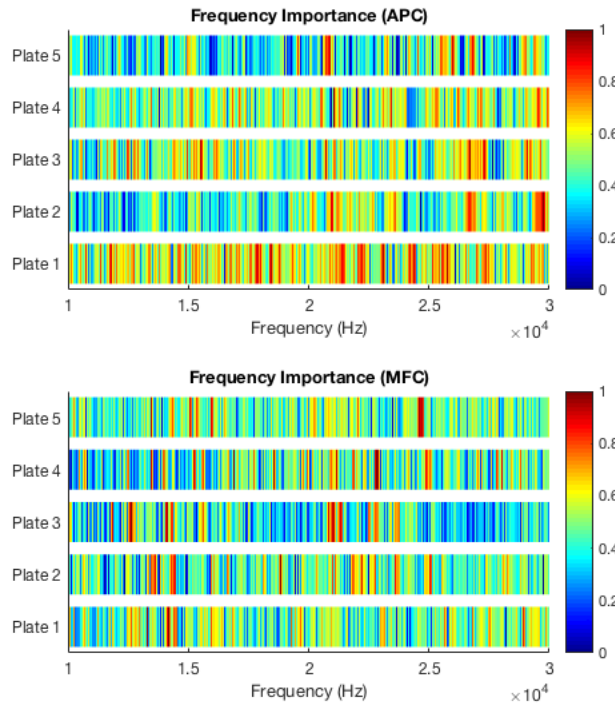


Figure 8. Frequency importance for each plate using random forest with 500 trees for low frequency range.

Using this problem formulation, the prediction accuracy using the APC data is 92%. It should be noted that the training data is included in this testing procedure because the baseline is required for estimating the model.

5. REGRESSION ANALYSIS

In this section, we present another formulation of the problem where instead of attempting to predict the discrete damage class, we attempt to predict the area of damage as a continuous variable. We believe this will improve performance because the discrete damage class might not represent the actual plate damage that occurred during testing, or not all impact events or resulting damages will be the same.

The image processing step is discussed in the next section but essentially, this damage metric was calculated for each plate impact by retrieving an amount of damage area from the image pixels or by the counting the pixels in the darker or damaged region.

5.1. Image Processing

Images were taken of the front and back of each plate before and after each impact. The images were taken at a constant height above each plate, with constant camera settings, including zoom and focus. Plate 1 was not used in the regression analysis because of inconsistencies in imaging.

Table 5. Impact damage area based on imaging.

Plate	Impact Damage (mm ²)				
	I1	I2	I3	I4	I5
1	N/A	N/A	N/A	N/A	N/A
2	11.0	20.9	33.8	47.6	73.2
3	7.0	15.3	31.2	41.7	60.7
4	12.7	18.9	34.2	49.3	55.7
5	10.0	19.5	34.7	43.7	57.7

The images from plates 2 through 5 were processed using MATLABs image processing toolbox following Alg.(1). The RGB images were first gray-scaled and then the gray color was inverted. This made the regions corresponding to damage lighter in color than the other non-damaged regions. The area of the damage region was captured using a threshold, which created a binary image. This threshold was created separately for each image using the average pixel value from the gray-scaled image. To ensure that the amount of plate damage in each image didn't alter this threshold, causing a bias based on the amount of plate damage, a box of white pixels was placed consistently over all regions of plate damage. Each plate's threshold was calculated based on the gray-scaled image that included this white box. This threshold was also tuned iteratively with the addition of a constant across all plate's by comparing the binary image to the original image for each plate and damage class until the captured region in the binary image well represented the actual damage.

The resulting binary images were further processed by filling in the regions that were fully enclosed by damage or active pixels using MATLABs "imfill" function. Noise was also cleaned using the "bwareaopen" function, which deletes active groups of connected pixels with less than a threshold of pixels. This threshold was determined iteratively to ensure that actual damage regions weren't deleted. The resulting damage or white pixels were counted for each plate and damage class image and then converted to mm² using a determined pixel to mm conversion. This final metric represents the actual damage area for each plate and impact damage. The resulting impact damage areas are shown in Tab. (5). This table shows that each impact results in a different damage area across the plates.

Note, the image specific threshold mentioned in this section was used because of inconsistencies in the plate images brightness, due to changes in ambient lighting.

5.2. Regression Results

The root-mean-square error (RMSE) between the predicted damage area and the actual damage area was calculated for each regression model. Three regression models using the same array function features from the full frequency range were evaluated, including a random forest regression model with 500 trees, a regression trees model, and a linear regres-

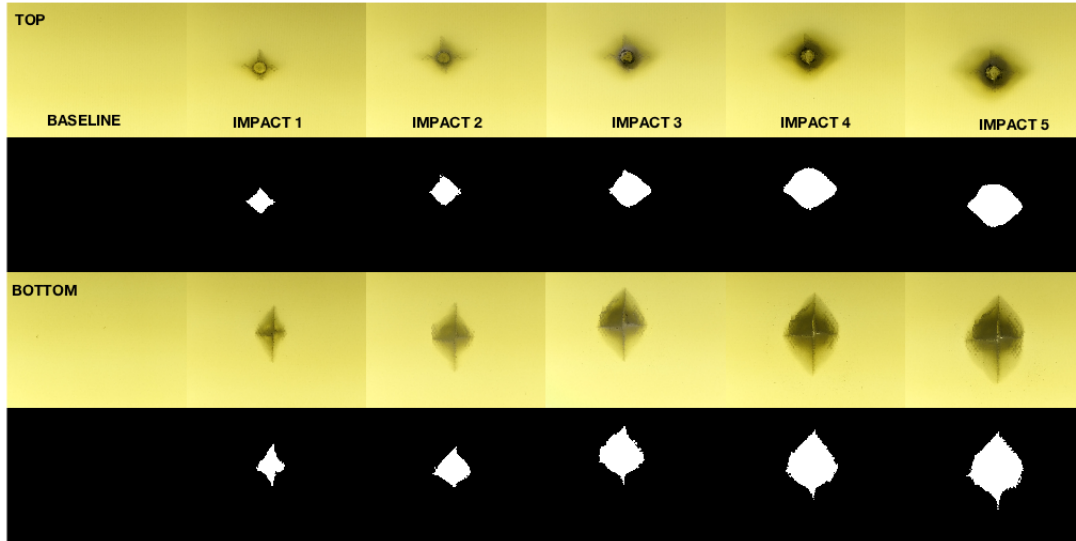


Figure 9. This figure shows the actual and binary images for each plate 4 impact, including the top and bottom plate images.

```

for each plate do
  for each damage class do
    for each plate orientation image (top and bottom) do
      convert RGB image to grayscale
      complement grayscale
      compute threshold value by taking mean pixel
      value of undamaged areas
      convert grayscale to binary image using image
      threshold value
      fill in enclosed regions using morphology
      "imfill" command
      filter the image to reduce noise using
      "bwareopen" command
      sum the damage pixels and convert to SI units
    end
  end
end

```

Algorithm 1: Image Processing

sion model. The RMSE results are shown in Tab. (6). The random forest regression model resulted in the lowest RMSE of 11.9 mm^2 , using the APC transducer data. This translates to 16.3% of the maximum damage area of 73.2 mm^2 . The regression trees model performs the second best, with a RMSE of 16.2 mm^2 , 22.1% of the maximum damage area, for the APC transducer data, and the linear regression model performs the worst with an RMSE of 27.0 mm^2 , 36.9% of the maximum damage area, for MFC transducer data.

6. DISCUSSION AND CONCLUSION

This multi-plate analysis tested the repeatability of machine learning algorithms to predict impact damage on a left-out or unknown plate. This study concludes that classification mod-

Table 6. Root mean square error for regression results.

	RMSE (mm^2)	
	APC	MFC
Random forest	11.9	19.2
Regression Trees	16.2	24.0
Linear model	27.0	36.3

els tested with a LOOCV method can produce high prediction accuracies of up to 78% with a random forest model. However, it is shown that these same classification models cannot accurately predict impact damage on a new plate, with the LOPOCV analysis resulting in only 43% accuracy using a classification tree.

These low multi-class results lead us to attempt a binary classification problem, in which the classes are baseline or impact. Using a Naive Bayes model, we achieved 92% accuracy.

The low accuracy in the multi-class results lead us to think of this as a regression problem, with the damage area of each impact as the response variable. The damage areas were calculated based on an imaging algorithm and show us that each impact results in a different amount of damage for each plate, further demonstrating that a regression analysis is needed. The regression analysis using the same features as the classification problem resulted in a RMSE of 11.9 mm^2 , or 16.3% of the maximum impact damage area, using a random forest regression model. The regression models may be better suited to damage predictions in which there is a continuous

amount of damage that can occur, rather than different types of damage predictions such as impact or fatigue damage.

6.1. Sources of Error

There are many sources of error during this multi-plate analysis. Each plate and transducer is slightly different because of manufacturing tolerances. This could account to different plate thickness, length, layering, and material quality and different transducer responses. There are also sources of error that result from our experimental setup such as transducer mounting, plate mounting to the aluminum frame, and inconsistencies during the drop tests. These errors could be caused by differences in plate drilled-hole locations, bolt torques, and impact damage locations. There are also environmental effects that could lead to errors such as the movement or vibrations near the plate while taking the impedance scans, changes in ambient temperature and humidity that may alter plate material mechanics, and changes in ambient lighting that could result in differences during imaging of impact damages. Follow-on studies will consider methods for limiting or quantifying these sources of error, and whether any can be compensated for, or ultimately removed from the experiment.

6.2. Future Work

In future work, we will complete further regression analysis on plate damage experiments, including both impact and fatigue damage experiments. Future experiments will involve research into the effects of plate geometry and curvature, the effect of the distance from the damaged area to the transducer, the effects of performing maintenance on composite plates, and the effects of exposing plates to sea water on predicting damage. We plan to predict more damage characteristics including shape and location metrics in a multivariate regression model.

Our future work will also investigate using other models to increase model accuracy and transferability across plates. The discovery of how different plates react to impact damage and their corresponding changes in their impedance response may require models that use transfer learning. Transfer learning is the ability of a system to use information gathered from learning one task and applying it to learning another novel task (Pan & Yang, 2010). In our case, the information gathered from learning how one plate's response changes due to damage could be used to create a model for predicting how another plate's response may change. In other ways, transfer learning could also be used to predict fatigue damage using the information gathered from predicting impact damage or vice versa.

REFERENCES

Antonio, F. d. O. (2010). Wave energy utilization: A review

- of the technologies. *Renewable and sustainable energy reviews*, 14(3), 899–918.
- Bishop, C. (2006). *Pattern recognition and machine learning*. Springer-Verlag New York.
- Breiman, L. (2001). Random forests. *Machine learning*, 45(1), 5–32.
- DOE. (2016). *U.S. department of energy wind and water power technologies office funding in the united states: Marine and hydrokinetic projects*.
- Dumoulin, C., Karaiskos, G., Sener, J.-Y., & Deraemaeker, A. (2014). Online monitoring of cracking in concrete structures using embedded piezoelectric transducers. *Smart materials and structures*, 23(11), 115016.
- EERE. (2017). *Wave energy prize*. Retrieved from <https://waveenergyprize.org/> (Online; accessed Aug-2017)
- Farinholt, K., Desrosiers, M., Kim, M., Friedersdorf, F., Adams, S., & Beling, P. (2016). Active sensing and damage classification for wave energy converter structural composites. In *Asme 2016 conference on smart materials, adaptive structures and intelligent systems*.
- Frieden, J., Cugnoni, J., Botsis, J., & Gmür, T. (2012a). Low energy impact damage monitoring of composites using dynamic strain signals from FBG sensors—Part II: Damage identification. *Composite Structures*, 94(2), 593–600.
- Frieden, J., Cugnoni, J., Botsis, J., & Gmür, T. (2012b). Low energy impact damage monitoring of composites using dynamic strain signals from FBG sensors—Part I: Impact detection and localization. *Composite Structures*, 94(2), 438–445.
- Lehmann, M., Karimpour, F., Goudey, C. A., Jacobson, P. T., & Alam, M.-R. (2017). Ocean wave energy in the united states: Current status and future perspectives. *Renewable and Sustainable Energy Reviews*.
- Nardi, D., Lampani, L., Pasquali, M., & Gaudenzi, P. (2016). Detection of low-velocity impact-induced delaminations in composite laminates using auto-regressive models. *Composite Structures*, 151, 108–113.
- Pan, S. J., & Yang, Q. (2010). A survey on transfer learning. *IEEE Transactions on knowledge and data engineering*, 22(10), 1345–1359.
- Park, G., & Inman, D. J. (2007). Structural health monitoring using piezoelectric impedance measurements. *Philosophical Transactions of the Royal Society of London A: Mathematical, Physical and Engineering Sciences*, 365(1851), 373–392.
- Pérez, M. A., Gil, L., & Oller, S. (2014). Impact damage identification in composite laminates using vibration testing. *Composite Structures*, 108, 267–276.
- Taylor, S. G., Farinholt, K., Choi, M., Jeong, H., Jang, J., Park, G., . . . Todd, M. D. (2014). Incipient crack detection in a composite wind turbine rotor blade. *Journal of Intelligent Material Systems and Structures*, 25(5),

613–620.

Xie, X., Xu, D., Guo, X., Sha, F., & Huang, S. (2016). Non-linear ultrasonic nondestructive evaluation of damaged concrete based on embedded piezoelectric sensors. *Research in Nondestructive Evaluation*, 27(3), 125–136.

Xu, D., Banerjee, S., Wang, Y., Huang, S., & Cheng, X. (2015). Temperature and loading effects of embedded smart piezoelectric sensor for health monitoring of concrete structures. *Construction and Building Materials*,

76, 187–193.

Yoon, J., He, D., & Van Hecke, B. (2015). On the use of a single piezoelectric strain sensor for wind turbine planetary gearbox fault diagnosis. *IEEE Transactions on Industrial Electronics*, 62(10), 6585–6593.

Yuce, M. I., & Muratoglu, A. (2015). Hydrokinetic energy conversion systems: a technology status review. *Renewable and Sustainable Energy Reviews*, 43, 72–82.